

## Full-length Article

# Mesenchymal stem cell-derived extracellular vesicles ameliorate inflammation-induced preterm brain injury



Karla Drommelschmidt<sup>a</sup>, Meray Serdar<sup>a</sup>, Ivo Bendix<sup>a</sup>, Josephine Herz<sup>a</sup>, Frederik Bertling<sup>a</sup>, Sebastian Prager<sup>a</sup>, Matthias Keller<sup>a</sup>, Anna-Kristin Ludwig<sup>b</sup>, Vikas Duhan<sup>c</sup>, Stefan Radtke<sup>b,d</sup>, Kyra de Miroschedji<sup>b</sup>, Peter A. Horn<sup>b</sup>, Yohan van de Looij<sup>e,f</sup>, Bernd Giebel<sup>b,\*</sup>, Ursula Felderhoff-Müser<sup>a,\*</sup>

<sup>a</sup> Department of Paediatrics I/Neonatology, University Hospital Essen, University of Duisburg-Essen, Essen, Germany

<sup>b</sup> Institute of Transfusion Medicine, University Hospital Essen, University of Duisburg-Essen, Essen, Germany

<sup>c</sup> Institute of Immunology, University Hospital Essen, University of Duisburg-Essen, Essen, Germany

<sup>d</sup> Clinical Research Division, Fred Hutchinson Cancer Research Centre, Seattle, WA 98109, USA

<sup>e</sup> Division of Child Growth and Development, Department of Paediatrics, University of Geneva, Geneva, Switzerland

<sup>f</sup> Laboratory of Functional and Metabolic Imaging, Ecole Polytechnique Fédérale de Lausanne, Lausanne, Switzerland

## ARTICLE INFO

## Article history:

Received 31 July 2016

Received in revised form 4 November 2016

Accepted 12 November 2016

Available online 12 November 2016

## Keywords:

Perinatal brain injury

Exosomes

Microvesicles

Extracellular vesicles

Mesenchymal stem cells

Inflammation

White matter injury

Lipopolysaccharide

## ABSTRACT

**Objective:** Preterm brain injury is a major cause of disability in later life, and may result in motor, cognitive and behavioural impairment for which no treatment is currently available. The aetiology is considered as multifactorial, and one underlying key player is inflammation leading to white and grey matter injury. Extracellular vesicles secreted by mesenchymal stem/stromal cells (MSC-EVs) have shown therapeutic potential in regenerative medicine. Here, we investigated the effects of MSC-EV treatment on brain microstructure and maturation, inflammatory processes and long-time outcome in a rodent model of inflammation-induced brain injury.

**Methods:** 3-Day-old Wistar rats (P3) were intraperitoneally injected with 0.25 mg/kg lipopolysaccharide or saline and treated with two repetitive doses of  $1 \times 10^8$  cell equivalents of MSC-EVs per kg bodyweight. Cellular degeneration and reactive gliosis at P5 and myelination at P11 were evaluated by immunohistochemistry and western blot. Long-term cognitive and motor function was assessed by behavioural testing. Diffusion tensor imaging at P125 evaluated long-term microstructural white matter alterations.

**Results:** MSC-EV treatment significantly ameliorated inflammation-induced neuronal cellular degeneration reduced microgliosis and prevented reactive astrogliosis. Short-term myelination deficits and long-term microstructural abnormalities of the white matter were restored by MSC-EV administration. Morphological effects of MSC-EV treatment resulted in improved long-lasting cognitive functions

**Interpretation:** MSC-EVs ameliorate inflammation-induced cellular damage in a rat model of preterm brain injury. MSC-EVs may serve as a novel therapeutic option by prevention of neuronal cell death, restoration of white matter microstructure, reduction of gliosis and long-term functional improvement.

© 2016 The Authors. Published by Elsevier Inc. This is an open access article under the CC BY-NC-ND license (<http://creativecommons.org/licenses/by-nc-nd/4.0/>).

## 1. Background

The rate of prematurely born infants has increased up to amounts of 10–12% of all live births attributable to late mother-

\* Corresponding authors at: Institute for Transfusion Medicine, University Hospital Essen, University Duisburg-Essen, Virchowstrasse 179, 45147 Essen, Germany (B. Giebel). Department of Paediatrics I, University Hospital Essen, University Duisburg-Essen, Hufelandstrasse 55, 45147 Essen, Germany (U. Felderhoff-Müser).

E-mail addresses: [bernd.giebel@uk-essen.de](mailto:bernd.giebel@uk-essen.de) (B. Giebel), [ursula.felderhoff@uk-essen.de](mailto:ursula.felderhoff@uk-essen.de) (U. Felderhoff-Müser).

<sup>1</sup> Equal contribution.

hood and infertility treatments (Beck et al., 2010; Mathews et al., 2011). Major progress in obstetric and neonatal care has significantly reduced mortality but more than 50% of survivors still remain at risk to suffer from long-term neurological sequelae. Beside severe motor impairment, cognitive disorders and neuropsychiatric problems including autism, attention deficit and hyperactivity disorders are often observed in long-term follow-up studies (Belmonte et al., 2004; Johnson et al., 2011; Wilson-Costello et al., 2005). Since the rate of severe cerebral palsy as a result from cystic periventricular leukomalacia has declined in recent years, diffuse cerebral white matter injury (WMI) is now the major type of brain damage (Benders et al., 2014). These subtle

changes caused by disturbed oligodendrocyte maturation are associated with altered development of the myelin sheath and consecutively altered cortical development leading to cognitive and behavioural deficits (Donega et al., 2014; Favrais et al., 2011).

According to the “multiple hit hypothesis”, a variety of noxious events such as fluctuations in oxygen supply caused by acute or chronic lung disease, drug exposure and inflammation may affect the developing brain and thereby result in cellular loss and maturation disturbances (Anjari et al., 2009; Brehmer et al., 2012; Cai et al., 2000; Felderhoff-Mueser et al., 2004; Kaindl et al., 2009). Predisposing factors for WMI are intrauterine and perinatal infections leading to systemic inflammation (Andrews et al., 1995; Hagberg and Mallard, 2005; Randis, 2010).

In preclinical studies, lipopolysaccharide (LPS) is used in experimental models to mimic the clinical situation (Brehmer et al., 2012; Eklind et al., 2001). In the clinical setting injurious stimuli may cause injury at different time points, making it difficult to identify the underlying insult. Therefore, neuroprotective treatments with preventive and/or regenerative properties are urgently needed. However, to date clinically applicable therapeutic options in preterm infants remain elusive.

Mesenchymal stem/stromal cells (MSCs) have been widely used in experimental and clinical paradigms such as stroke (Hess and Hill, 2011; Mendez-Otero et al., 2007), multiple sclerosis (Gerdoni et al., 2007; Orack et al., 2015), cardiovascular diseases (Williams and Hare, 2011), and graft-versus-host disease (Baron and Storb, 2011; Le Blanc et al., 2004). Preclinical studies using models of birth asphyxia and preterm white matter injury confirmed the neuroprotective capacities of MSCs after local, systemic or even intranasal application (Ohshima et al., 2015; van Velthoven et al., 2013; Wei et al., 2015). Beneficial effects were observed, independently of whether autologous or allogenic MSCs were administered. According to their multiple differentiation capabilities MSCs were initially thought to home to affected tissues, replace lost or damaged cell types and modulate immune responses (Bianco et al., 2013; Wang et al., 2014). In recent years, however, increasing evidence suggests that their therapeutic effects are rather mediated in a paracrine manner (Gnecchi et al., 2005; Hsieh et al., 2013; Lee et al., 2009) mainly being mediated by extracellular vesicles (EVs), such as exosomes and microvesicles (Börger et al., 2016; Bruno et al., 2009; Doepfner et al., 2015; Kordelas et al., 2014; Lai et al., 2010; Lener et al., 2015).

EVs are naturally occurring membrane-surrounded vesicles and released by almost all cell types into the extracellular environment. Exosomes, derivatives of the late endosomal compartment (70–150 nm), and microvesicles, bud offs of the plasma membrane (100–1000 nm), are the most prominent EV types. Both are assembled in cell type specific manners containing specific cargo combinations of lipids, RNA, cell-adhesion-molecules, cytokines, and other proteins. They mediate intercellular communication processes and transmit tailored information to specific target cells (Ludwig and Giebel, 2012; Yanez-Mo et al., 2015). According to their unique features, EVs provide promising tools in immune and regenerative therapies and may also be used for targeted drug delivery (Lener et al., 2015). In contrast to cells, they lack any endogenous tumour-formation potential and are easier to handle. Furthermore, due to their small size they can be sterilized by filtration (Lener et al., 2015).

Here, we hypothesised that MSC-EV treatment yields therapeutic potential for preterm white matter injury. Using an established rodent model of perinatal inflammation, early effects on cellular degeneration, reactive gliosis, and myelination were analysed. Long-term structural alterations of the white matter were characterized by diffusion tensor imaging and behavioural testing.

## 2. Material and methods

### 2.1. Expansion and characterization of MSCs

MSCs were raised from bone marrow (BM) samples of anonymised human donors following informed consent according to the Declaration of Helsinki as previously described. Briefly BM-derived mononuclear cells were harvested by Ficoll (Biocoll Separating Solution; Biochrom AG Berlin Germany) density gradient centrifugation and seeded at a density of  $2 \times 10^6$  cells per well into 6-well tissue culture plates containing MSC basal media (Pan-Biotech Aidenbach Germany) supplemented with 10% human thrombocyte lysate 1% glutamine and 1% penicillin-streptomycin (Invitrogen Darmstadt Germany). After 24 h non-adherent cells were removed by medium exchange. After reaching confluence cells were continuously passaged. MSCs were characterized by flow cytometry and tested for their differentiation potential (Doepfner et al., 2015; Kordelas et al., 2014).

### 2.2. Enrichment of EVs from conditioned MSC media

After passage 3, MSC conditioned media (CM) were harvested every 48 h, passed through a 0.22  $\mu\text{m}$  filter membrane (TPP TechnoPlastic Products AG, Trasadingen, Switzerland) to remove cell debris and larger vesicles and stored at  $-20^\circ\text{C}$ . After thawing, CMs were centrifuged at  $10,000 \times g$  in an Avanti J-26 XP centrifuge (Beckmann Coulter, Germany) for 30 min. Subsequently, EVs within supernatants were concentrated by a polyethyleneglycol (PEG) precipitation method (Kordelas et al., 2014). Briefly, PEG6000 (50% wt/vol; Sigma-Aldrich, Taufkirchen, Germany) and NaCl were added to a final concentration of 10% PEG and 75 mM NaCl and incubated for 8–12 h at  $4^\circ\text{C}$ . EVs were concentrated by centrifugation for 30 min at  $1500 \times g$ . To reduce the amount of co-precipitated proteins pellets were resolved in normal saline (B. Braun Melsungen, Melsungen, Germany) to a total volume of 45 ml; EVs were re-precipitated by ultracentrifugation for 2 h at  $110,000 \times g$  in an Optima L7-65 ultracentrifuge using the tight angle rotor Ti45 (Beckman Coulter). EV pellets were diluted in saline to a concentration of  $4 \times 10^7$  cell equivalents/1 ml. Aliquots were stored at  $-80^\circ\text{C}$  until usage. EV samples were characterized by Nanoparticle Tracking Analyses (NTA) (Sokolova et al., 2011) on the ZetaView platform (Particle Metrix, Meerbusch, Germany). The presence of exosomal marker proteins (Tsg101 or CD81) was confirmed by western blot. Samples were tested for contamination with HIV-1, HIV-2, HCV and HBV by multiplex PCR using the Procleix Ultrio Elite kit (Grifols Deutschland GmbH, Frankfurt am Main, Germany). To test for microbiological contamination 100  $\mu\text{l}$  of each EV sample were diluted with saline to a total volume of 1 ml. Subsequently the diluted EV solution was inoculated into BactAlert bottles (bioMérieux, Nürtingen, Germany). Bottles were incubated at  $32 \pm 1^\circ\text{C}$  for 14 days, and automatic readings were taken every 10 min. All samples used were negative in all assays.

### 2.3. Experimental animals

All animal procedures were performed in accordance with the international guidelines for good laboratory practice and the institutional guidelines of the University Hospital Essen approved by the animal welfare committees of North Rhine Westphalia. Pups were kept under a 12 h light/dark cycle and had free access to food and water after separation from their dams. All groups were sex- and weight matched.

3-Day-old (P3) Wistar rat pups were randomly assigned to treatments. Pups were equally distributed to control for maternal care. Four experimental groups were treated with intraperitoneal

(i.p.)-injections (lower abdomen, both sides) as follows: (1) vehicle (saline NaCl 0.9%); (2) vehicle and MSC-EVs ( $1 \times 10^8$  cell equivalents/kg bodyweight) at 3 h before and 24 h after vehicle injection; (3) LPS 0.25 mg/kg (*E. coli* O55:B5, Sigma-Aldrich, Steinheim, Germany; in saline with a volume of 0.01 ml/g); (4) LPS and MSC-EVs at 3 h before and 24 h after a single LPS injection.

In total, 173 pups (saline (1):  $n = 45$ , MSC-EV (2):  $n = 38$ , LPS (3):  $n = 46$ , LPS/MSCEV (4):  $n = 44$ ) derived from 14 litters were enrolled. Rats were sacrificed at P5, P11 and P125. In the first set of experiments 85 rats were used to assess apoptosis, micro- and astrogliosis via western blot and immunohistochemistry on P5 (saline (1):  $n = 21$ , MSC-EV (2):  $n = 20$ , LPS (3):  $n = 22$ , LPS/MSCEV (4):  $n = 22$ ). These animals were also used for quantification of pro-inflammatory plasma and cerebral cytokine levels. A second cohort was used for western blot analysis and qualitative evaluation of myelin basic protein (MBP) expression on P11 (saline (1):  $n = 15$ , MSC-EV (2):  $n = 10$ , LPS (3):  $n = 14$ , LPS/MSCEV (4):  $n = 12$ ). In accordance with previous studies of our group cellular degeneration was determined at P5 and myelination at P11 (Brehmer et al., 2012; Felderhoff-Mueser et al., 2004).

A third set of experimental animals was used for behavioural testing (saline (1):  $n = 9$ , MSC-EV (2):  $n = 8$ , LPS (3):  $n = 10$ , LPS/MSCEV (4):  $n = 10$ ). Out of these, brains of 6 animals of each experimental group were subjected to diffusion tensor imaging on P125. Animals subjected to behavioural testing and DTI were weaned at P21 and housed in groups of 4–5 animals per cage. Bodyweight as a sign for general health was recorded at P3, P4, P5, P11 and once a week after the weaning period for behavioural studies. Neurodevelopmental outcome was assessed from P30 and P90. Post-mortem Diffusion Tensor-Magnetic Resonance Imaging (DT-MRI) was carried out at P125 to evaluate long-term microstructural white matter changes. For western blot analysis, pups were transcardially perfused with phosphate buffered saline (PBS), the olfactory bulb and the cerebellum were removed, and brain hemispheres and white matter enriched fractions (including corpus callosum, deep cortical white matter and external capsule) were snap-frozen in liquid nitrogen and stored at  $-80^\circ\text{C}$  until further analysis. Whole hemispheres were used for western blot for overall evaluation of myelination. To correlate specific effects on myelination with local inflammatory reactions white matter enriched fractions were used as previously described (Serdar et al., 2016). For histological analysis pups were transcardially perfused with PBS followed by 4% paraformaldehyde (PFA, Sigma-Aldrich). Brains were removed and post-fixed in 4% PFA overnight at  $4^\circ\text{C}$  and embedded in paraffin. MRI brains were post-fixed in 4% PFA for four days and stored in 1% PFA until further analysis.

#### 2.4. Immunoblotting

Snap-frozen hemispheres (for analysis of MBP) or white matter enriched fractions were homogenized in ice-cooled radioimmunoprecipitation assay (RIPA) buffer, supplemented with phenylmethanesulfonyl fluoride (PMFS, Sigma-Aldrich) and complete Mini, EDTA-free (Roche, Basel, Switzerland). Homogenates were centrifuged at 3000g for 10 min followed by 17,000g for 20 min. Protein concentrations in the remaining cytosolic extracts were determined using the BCA assay kit (Thermo Fisher Scientific, Dreieich, Germany). Lysates were denatured in Laemmli sample buffer at  $95^\circ\text{C}$  for 10 min and separated by 15% or 8% sodium dodecyl sulfate polyacrylamide gel electrophoresis, followed by blotting onto nitrocellulose membranes (0.2  $\mu\text{m}$  or 0.4  $\mu\text{m}$  pore, Protran, Sigma-Aldrich). Equal loading and transfer of proteins was confirmed by staining of membranes with Ponceau S solution (Sigma-Aldrich). 5% non-fat dry milk in Tris buffered saline/0.1% Tween 20 (TBST) was used for blocking nonspecific protein binding at room temperature for 60 min. Membranes were incubated over-

night ( $4^\circ\text{C}$ ) with the primary antibody in 5% non-fat dry milk in TBST. The following primary antibodies were used: rabbit-anti-cleaved Caspase 3 (cCaspase 3 1:1000, Cell Signaling Technology, Boston, USA), rabbit-anti-Iba1 (1:1000, Wako Pure Chemical Industries, Osaka, Japan), mouse-anti-MBP antibody (1:10,000, Abcam, Cambridge, UK) and mouse-anti-glial fibrillary acidic protein (GFAP) (1:500, Covance, Münster, Germany). Horseradish peroxidase-conjugated secondary antibodies directed against the specific host species were used for detection. Signals were visualized using enhanced chemiluminescence (ECL; GE Healthcare Europe GmbH, Freiburg, Germany) and quantified using the ChemiDoc XRS+ imaging system and Image Lab software (Bio-Rad, Munich, Germany).

#### 2.5. Immunohistochemistry

Terminal deoxynucleotidyl transferase-mediated biotinylated UTP nick end labelling (TUNEL) assays were performed on 10  $\mu\text{m}$  coronal paraffin sections according to the manufacturer's instructions (In Situ cell death detection kit, FITC; Roche) at P5. After deparaffinisation, coronal sections ( $-3.72 \pm 0.5$  mm) were rehydrated. Antigen-retrieval was carried out in a pre-heated 10 mM sodium-citrate buffer (pH 6,0) for 30 min. Sections were blocked with 1% bovine serum albumin (Fraction V), 0.3% cold fish skin gelatine and 0.1% Tween 20 (all Sigma-Aldrich) in Tris-buffered-saline. For analysis of myelination, microglia and astrocytes sections were incubated with primary antibodies (mouse anti-MBP (1:100, SMI-99, BioLegend, Sternberger Monoclonals, San Diego, USA), mouse anti-CD68 (1:100, AbD Serotec, Puchheim, Germany), rabbit anti-Iba-1 (1:500, Wako), mouse anti-GFAP (1:100, Covance)) overnight at  $4^\circ\text{C}$ , followed by secondary antibody incubation (anti-mouse Alexa Fluor 488, anti-rabbit Alexa Fluor 488, anti-mouse Alexa Fluor 555, 1:500 Invitrogen, Darmstadt, Germany) for 1 h at room temperature. For nuclear staining sections were incubated for 10 min with 4',6-Diamidin-2-phenylindol (DAPI, 100 ng/mL; Invitrogen). Slides were mounted with Fluorescent Mounting Medium and kept in the dark at  $4^\circ\text{C}$ .

#### 2.6. Analysis of pro-inflammatory cytokines

For analysis of cytokines in serum, blood was collected from the right atrium before perfusion. Serum was prepared after clotting in uncoated tubes by centrifugation at 3000g for 5 min. Cytokines were determined using Bio-Plex Pro™ Rat Cytokine Assay (Bio-Rad). Data were acquired with Luminex 200 and IS2.3/xPONENT3.1 software and further processed with the R package nCal. Standard curves were fitted by logistic regression to estimate absolute concentration of analytes.

Cerebral cytokines were measured using real time PCR. Total RNA was isolated from snap-frozen tissue by acidic phenol/chloroform extraction (peqGOLD RNAPure™; PEQLAB Biotechnologie, Erlangen, Germany) and 4  $\mu\text{g}$  of RNA were reverse transcribed. Gene expression analysis was performed as previously described using the StepOne plus (Applied Biosystems, Foster City, CA, USA (Brehmer et al., 2012)). The PCR products of interleukin 1 $\beta$  (IL-1 $\beta$ ), tumor necrosis factor  $\alpha$  (TNF- $\alpha$ ), interleukin 18 (IL-18) and  $\beta$ -actin (as internal standard) were quantified in real time, by fluorogenic reporter oligonucleotide probes and primers (Biotex, Berlin, Germany). Sequences and corresponding GenBank accession numbers are provided in Supplemental Table 1. Real-time PCR and detection were performed in duplicates, measurements repeated 2 times for each sample. Target gene expression was quantified according to the  $2^{-\Delta\Delta\text{CT}}$  method.

IL-1 $\beta$  protein expression was analysed in brain lysates using an IL-1 $\beta$  ELISA kit (R&D Systems, Wiesbaden, Germany) according to the manufacturer's instructions.

## 2.7. Confocal microscopy and analysis

Brain sections were analysed by confocal microscopy (A1plus, Eclipse Ti, with NIS Elements AR software, Nikon, Düsseldorf, Germany). Optical sections were acquired with a field depth of 10  $\mu\text{m}$  (1  $\mu\text{m}$  steps), using a 20x objective (Nikon N, Plan Apo VC 20x/0.75) and the NIS Elements AR Software. Two different filters (DAPI (450/50–405 LP), Alexa Fluor 488 (515/20–540 LP)) were used for image acquisition. For analysis of TUNEL-stained sections, images of two regions of interest (ROI, each: 396,900  $\mu\text{m}^2$ ), in white matter and cortex were acquired. TUNEL-positive cells were counted by a blinded observer in two sections per animal and ROI. For MBP staining complete hemispheres were scanned with a 10x objective (Nikon N, Plan Apo, 10x/0.45). For analysis of astro- and microgliosis, two ROIs in the cingulate white matter and the internal capsule were chosen as predominantly susceptible to LPS-induced micro- and astrogliosis. The total number of CD68 and Iba-1 positive cells was counted in these ROIs (total area: 585,900  $\mu\text{m}^2$ ) and the number of cells/ $\text{mm}^2$  was calculated. Since GFAP staining revealed densely packed networks of positive fibres in LPS-treated animals not allowing counting of single cells, the positively stained area was analysed as previously described (Schafer et al., 2012; Sullivan et al., 2010) using the binary tool of NIS AIR software (Nikon, Germany).

## 2.8. Behavioural studies

Animals were transferred to the behavioural unit one week in advance of testing in order to familiarise them with the investigator and an inverted 12 h light/dark cycle. Behavioural testing with all tests applied was performed in every animal starting at P30 in adolescent and repeated from P90 in adult animals. We mainly focused on assessment of cognitive function because clinical data provide convincing evidence that long-term cognitive function is impaired in a significant number of preterm infants (Marlow et al., 2015). Based on these clinical indications combined with recent experimental studies reporting a cognitive deficit after an inflammatory stimulus (Favrais et al., 2011) we performed two different cognitive tests (*Barnes Maze* and *Novel Object Recognition*). To rule out potential confounding effects by motoric impairment or anxiety-related behaviour the *Open Field* test was applied.

One day of *Open Field* was followed by *Novel Object Recognition* for 4 days and *Barnes Maze* for 4 days. Experiments were carried out during the active phase. Data were recorded by using an automatic tracking system (Video-Mot2, TSE Systems, Bad Homburg, Germany) and exported for statistical analysis. The *Open Field* was used to assess spontaneous motor-activity and anxiety-related behaviour (DeFries et al., 1966; Karen et al., 2013). Animals were placed in the centre of an *Open Field* arena (50  $\times$  50  $\times$  40 cm), upon an infrared (IR) light-box (TSE Systems) emitting IR light (850 nm) for 5 min. Activity parameters such as total distance and velocity were analysed. Non-spatial, non-aversive memory functions were assessed with *Novel Object Recognition* which relies on the observation, that animals preferentially explore novel objects over those that are familiar (Chambon et al., 2011). For the *Novel Object Recognition* test, the time of direct head contacts with the objects was recorded by the automated tracking system Video-Mot2 (TSE Systems).

At the start of the experiment animals were placed in the centre of the Y-maze and movements were recorded by a tracking system. On the first day animals were habituated to the Y-maze without objects followed by 2 training days with identical objects in each arm of the maze. At day 4 a novel object was changed in one arm and the time spent with familiar and novel objects were recorded. Testing time per session was 5 min and the first minute was used for quantification (Chambon et al., 2011). For *Barnes Maze*

animals were placed in the centre of the maze (1.22 m width, 0.8 m height, 20 holes at the border, TSE Systems) in a glass cylinder under red light. Light was switched to bright light to provide extra-maze cues as aid to orientation. After removing the cylinder (30 s under bright light) the animal was allowed to explore the maze and find the escape box within 120 s, where they were left for 1 min. Animals who did not find the escape box were gently placed into it for 1 min. To avoid intra-maze cues, such as material surface or odour, the escape box was clockwise rotated for every other animal, with the same escape location for each animal at the three training days. We applied a training period for 3 days, only, since our previous analyses revealed that all experimental groups reached a similar level of latency to find the trained escape box after three days in another model of preterm brain injury (Serdar et al., 2016). To test adaptive memory function the spatial probe test was applied on the fourth day by closing all holes i.e. animals had to adapt to an altered environment which may lead to increased latencies to find the trained escape hole (O'Leary et al., 2011).

## 2.9. Diffusion tensor-magnetic resonance imaging (DT-MRI)

Postmortem DT-MRI acquisition was performed in fixed brains from animals sacrificed at P125. All experiments were performed on an actively shielded horizontal 9.4T/31 cm magnet (Varian/Magnex) equipped with 12 cm gradient coils (400 mT/m, 120  $\mu\text{s}$ ) with a transceiver 25 mm birdcage volume RF coil. A spin echo sequence with addition of the Stejskal-Tanner diffusion gradients was used. Diffusion gradients were applied along six spatial directions: dual gradient diffusion gradient sampling scheme. Intensity, duration and diffusion time were set to 22 G/cm, 3 ms and 20 ms respectively, given a b-value of 1185  $\text{s}/\text{mm}^2$ . A field of view of 16  $\times$  16  $\text{mm}^2$  was sampled on a 128  $\times$  64 cartesian grid. Multi-slice DT images were acquired (12 slices of 0.5 mm thickness) in the axial plane with 10 averages and TE/TR = 30/2000 ms. Using an in house Matlab script (Mathworks, Natick, MA, USA), the radial diffusivity ( $D_{\perp}$ ), the axial diffusivity ( $D_{\parallel}$ ), the mean diffusivity (MD) as well as fractional anisotropy were derived from the tensor. The program allows manual delineation of the ROI on the fractional anisotropy maps. For quantification the corpus callosum was analysed.

## 2.10. Statistical analysis

Prism 6 (GraphPad Software, San Diego, USA) was used for data presentation and statistical analysis. Differences between groups were determined by two-way analysis of variance (two-way ANOVA) or three-way ANOVA (for learning behaviour) followed by Tukey's post hoc test for multiple comparisons. For MRI results, nonparametric Mann-Whitney test was used. P-values less than 0.05 were considered as statistically significant.

## 3. Results

To study the potential therapeutic impact of MSC-EVs in LPS induced perinatal brain injury rats were treated with systemic injections of either LPS or MSC-EVs or an application of both treatments. There were no significant differences in weight gain between experimental groups (data not shown). Out of 90 LPS-treated animals (LPS and LPS/MS-C-EV) one died in the LPS vehicle group. No obvious side effects were detected. Furthermore, there were no significant gender differences in our experiments.

### 3.1. MSC-EV treatment decreases LPS-mediated cellular degeneration in the immature brain

Systemic application of LPS causes cellular degeneration and apoptosis in the developing rat brain (Brehmer et al., 2012; Lodygensky et al., 2014). To analyse the effect of MSC-EV treatment inflammation-induced brain injury, cellular degeneration was measured via western blot of cCaspase 3 protein expression in tissue preparations of cortex and white matter at 48 h after LPS application (i.e. 24 h after the second MSC-EV injection, P5). LPS treatment led to a marked increase in cCaspase 3 expression, which was significantly reduced by MSC-EV treatment (Fig. 1A). To verify these results, immunohistochemistry was used to examine cell death in cortex and white matter revealing a significant LPS-induced increase of TUNEL-positive cells in both brain regions. This LPS-induced increase of TUNEL-positive cells was significantly reduced upon treatment with MSC-EVs, in both, cortex and white matter (Fig. 1B and C).

### 3.2. MSC-EVs prevent reactive gliosis after inflammation-induced perinatal brain injury

Since systemic LPS administration at P3 has been described to trigger microglia activation and a strong induction of astrogliosis (Lodygensky et al., 2014) the immunomodulatory effect of MSC-EVs alone and after application of LPS was analysed 48 h after LPS injection (i.e. 24 h after the last EV administration). Microgliosis was determined by western blot and immunohistochemistry of Iba-1 and CD68, respectively. Compared to the saline treated control group, LPS treatment resulted in a significant increase of Iba-1 and CD68 positive cells and Iba-1 protein expression in white matter-enriched brain fractions (Fig. 2A, B, D Supplemental Fig. S1A). Co-treatment with MSC-EVs significantly reduced microglia cell numbers and Iba-1 protein expression (Fig. 2A, B and D). There was a marked but non-significant decrease in the number of CD68 positive cells upon MSC-EV treatment in LPS exposed animals. Circularity was significantly reduced by a combination of both LPS and MSC-EV treatment (Supplemental Fig. S1 A and B). Reactive astrogliosis was determined by immunohistochemistry and western blot analysis of GFAP. A densely packed network of GFAP positive fibres and hypertrophic somata was observed in LPS treated animals (Fig. 2A). Quantification of GFAP positive area revealed a significant LPS response, which was ameliorated upon MSC-EV co-treatment (Fig. 2C). These results were confirmed by western blot analysis (Fig. 2E). Overall statistical analysis (two-way ANOVA) of micro- and astrogliosis (Fig. 2) demonstrated significant interaction effects between EVs and LPS (Iba-1:  $F(1,24) = 46.75$ ,  $p < 0.001$ ; GFAP:  $F(1,24) = 4.85$ ,  $p < 0.05$ ), indicating that EVs are particularly active in the case of LPS-induced inflammation.

## 4. Modulation of pro-inflammatory cytokines by LPS and MSC-EV treatment

Systemic and cerebral pro-inflammatory cytokine responses were measured in serum and brain 24 h after the last MSC-EV-injection (Fig. 3, Supplemental Fig. C and D). This specific time point was chosen to correlate findings with our read-outs on cerebral apoptosis, micro- and astrogliosis (Figs. 1 and 2). Modest effects on TNF $\alpha$  and IL-18 expression by LPS and MSC-EV treatment were detected in serum and brain (Supplemental Fig. S1C and D). However, IL-18 mRNA and protein expression were markedly increased in the brain whereas circulating IL-1 $\beta$  levels were not affected (Fig. 3). MSC-EV treatment apparently did not affect cytokine expression in the current experimental setting.

### 4.1. LPS-induced hypomyelination is ameliorated by MSC-EV treatment in the developing brain

One consequence of inflammation-induced brain injury is hypomyelination of white matter tracts (Brehmer et al., 2012; Favrais et al., 2011). MBP served as a marker for myelination processes and was assessed by western blot and immunohistochemistry at P11. As shown in representative images in Fig. 4A, LPS treatment resulted in a decrease of MBP protein expression which was restored by co-treatment with MSC-EV (Fig. 4A). Quantification of protein lysates by western blot analysis isolated from whole hemispheres confirmed these qualitative observations at P11 and revealed significantly increased levels of MBP expression in MSC-EV treated animals (Fig. 4B). Analysis of MBP expression at P11 by two-way ANOVA revealed main effects by LPS ( $F(1,47) = 7.77$ ,  $p < 0.01$ ) and MSC-EVs ( $F(1,47) = 20.55$ ,  $p < 0.001$ ) but no interaction effects.

### 4.2. MSC EV treatment improves long-term cognitive deficits after inflammatory brain injury

To evaluate long-term effects of MSC-EV treatment on cognitive function and motor activity after inflammation-induced brain injury we tested adolescent (P30) and adult (P90) rats. General motor activity and anxiety-related behaviour was assessed by *Open Field* and revealed that neither LPS nor MSC-EV treatment altered activity and anxiety parameters of adolescent and adult rats (Fig. 5A–C). *Barnes Maze* revealed that learning behaviour is not affected by MSC-EVs or LPS treatment as three-way ANOVA only revealed a main effect for time ( $F(2,99) = 20.75$ ,  $p < 0.001$ ). All animals showed the same improvement over time independent of treatment (Fig. 6A, B). However, the spatial probe test as an indicator for adaptive memory function performed at the fourth day (Fig. 6C) demonstrated main effects by LPS ( $F(1,33) = 8.30$ ,  $p < 0.01$ ), shown by an impaired latency to find the trained hole. Co-treatment with MSC-EVs significantly improved this memory deficit to control levels in adolescent and in adult animals (Fig. 6C). In adolescent rats the protective effect of MSC-EV treatment observed by *Barnes Maze* for spatiotemporal memory function was also proven in the *Novel Object Recognition* test, demonstrating a reduced exploratory activity at the novel object in adolescent rats upon neonatal LPS exposure. This indicator for non-spatial, non-aversive memory function was significantly improved to control levels by MSC-EV treatment (Fig. 6D).

### 4.3. MSC-EVs restore long-term microstructural white matter alterations after perinatal inflammation-induced brain injury

To evaluate whether the observed cognitive deficits correlated with alterations of white matter structures, DT-MRI was obtained from post-mortem P125 rat brains. In addition to ventricular enlargement after LPS injection, which was ameliorated by MSC-EV treatment (Fig. 7A), fractional anisotropy as a measure of white matter integrity was significantly decreased in the corpus callosum after neonatal LPS exposure (Fig. 7B). In LPS exposed animals fractional anisotropy was significantly increased almost to control levels following MSC-EV treatment (Fig. 7B). The observed LPS-induced fractional anisotropy decrease was related to an increase of radial diffusivity ( $D_{\perp}$ ), which can be generally attributed to myelination defects (Song et al., 2002). Of note, MSC-EV co-treatment significantly reduced radial diffusivity compared to LPS treatment only (Fig. 7C).

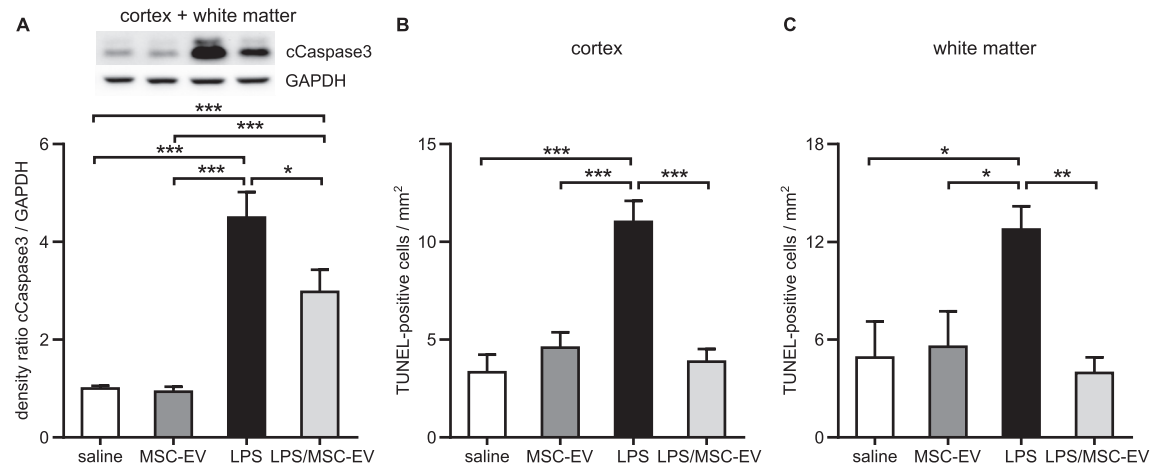


**Fig. 1.** LPS-induced cellular degeneration is ameliorated by MSC-EVs. Systemic inflammation was induced in P3 rat pups by i.p. injection of 0.25 mg/kg LPS. MSC-EVs were administered i.p. at 3 h before and 24 h after LPS-injection. Cellular degeneration was assessed at P5 by western blot analysis and immunohistochemistry (A–C). Cellular degeneration was determined by cCaspase 3 protein expression in white matter-enriched protein lysates including cortex and white matter of the corpus callosum, deep cortical white matter, and external capsule (A,  $n = 12$ –15 per group). Quantification of TUNEL-positive cells derived from immunohistochemistry in cortex and in white matter structures (B and C,  $n = 6$ –8 per group). Data are presented as mean + SEM.  $p < 0.05$ ,  $^{*}p < 0.01$ ,  $^{***}p < 0.001$ .

## 5. Discussion

Due to the multifactorial origin of preterm brain injury affecting the developing organism at different perinatal time points, no single therapy has proven effective for prevention and/or treatment. Stem cell based approaches attracted particular interest because of their ease of isolation, characterization, proposed multipotency and pleiotropic effects yielding the potential to treat this complex disease.

The present study investigated the therapeutic and regenerative potential of MSC-EVs in the developing central nervous system with special emphasis on white matter injury. In our experimental rodent model of inflammation-induced preterm brain injury at P3, systemic i.p. MSC-EV application effectively reduced cellular degeneration, modulated inflammatory responses and decreased early LPS-induced micro- and astrogliosis. As a consequence from a modulation of the acute response, MSC-EVs significantly improved LPS-induced hypomyelination and long-term cognitive deficits in rats up to adulthood. MRI analyses at adult age (P125) confirmed MSC-EV treatment-induced structural effects in LPS exposed animals as fractional anisotropy in white matter structures was significantly restored almost to control levels. No side effects such as weight loss, clinical illness or death were detected in experimental animals, indicating a good tolerance of MSC-EVs.

Our findings are largely in line with previous studies on the application of MSC-EVs in adult models of acute cerebral tissue damage, such as acute stroke and traumatic brain injury demonstrating positive effects on inflammatory responses, neuroprotection, angiogenesis, neurogenesis and thereby improved long-term neurological function (Doepfner et al., 2015; Xin et al., 2013; Zhang et al., 2015).

With MSC treatment similar effects have been observed in the developing brain. In rodent models of hypoxic-ischemic injury, representing birth asphyxia in term born infants (van Velthoven et al., 2011), and in an ovine model of global intrauterine hypoxia-ischemia (Jellema et al., 2013) systemic application of MSCs provided neuroprotection by reduction of cell death, inflammation and repair. The hypothesis that EVs are potentially equivalent to MSCs is strengthened by the fact that in adult disease models including ischemic stroke and acute kidney failure, EVs derived from MSC conditioned medium were as effective as treatment with the cells themselves (Bruno et al., 2009; Doepfner et al.,

2015). In neonatal rats subjected to hypoxic-ischemic injury, conditioned medium of adipose-derived stem cells containing EVs significantly protected against hippocampal and cortical volume loss and improved functional outcome at the age of eight postnatal weeks (Wei et al., 2015). Findings of the present study are supported by recent observations of MSC-EV treatment in an ovine model of intrauterine hypoxia-ischemia. Systemic application of MSC-EVs to foetuses one hour and four days after induction of global umbilical cord ischemia restored brain function by reduction of seizure burden and preservation of baroreceptor reflex sensitivity (Ophelders et al., 2016). However, only a tendency to morphological improvement was observed, possibly explained by the different experimental models and species used. Alternatively, the quality of MSC-EVs, their concentration or the application protocol might not have been optimal in this experimental setting. Thus, it will be important to study optimized MSC-EV production and treatment schemes in the various experimental models.

The present study focussed on preterm white matter injury, since myelination is the key to functional activity of axons, allowing them to connect to neurons and strengthen circuitry throughout the nervous system (de Hoz and Simons, 2015). Using fractional anisotropy as a marker for tissue microstructure alterations, clinical studies revealed that cognitive and motor deficits in preterm born infants can be directly related to morphological abnormalities in particular in white matter regions (Counsell et al., 2008). Experimental studies including our own demonstrated that LPS administered in rodents at P3 resulted in a significant decrease of fractional anisotropy and in an increased radial diffusivity at P21 in post-mortem *ex vivo* analyses (Brehmer et al., 2012). Our results revealed that this decrease in fractional anisotropy also persists into full adulthood (P125). Neonatal treatment with MSC-EVs restored fractional anisotropy, possibly contributing to the normalized cognitive capacities of experimental animals at adolescent and adult age.

Whereas in adult rats peripherally administered LPS has been shown to cause spatial learning deficits assessed by water maze (Shaw et al., 2001) we did not observe alterations of learning behaviour which closely resembles results from our previous study in another preterm brain injury model of oxygen-induced brain injury (Serdar et al., 2016). However, a memory deficit has been described after mild systemic inflammation induced by IL1 $\beta$ -injection between P1 and P5, but not between P6 and P10,

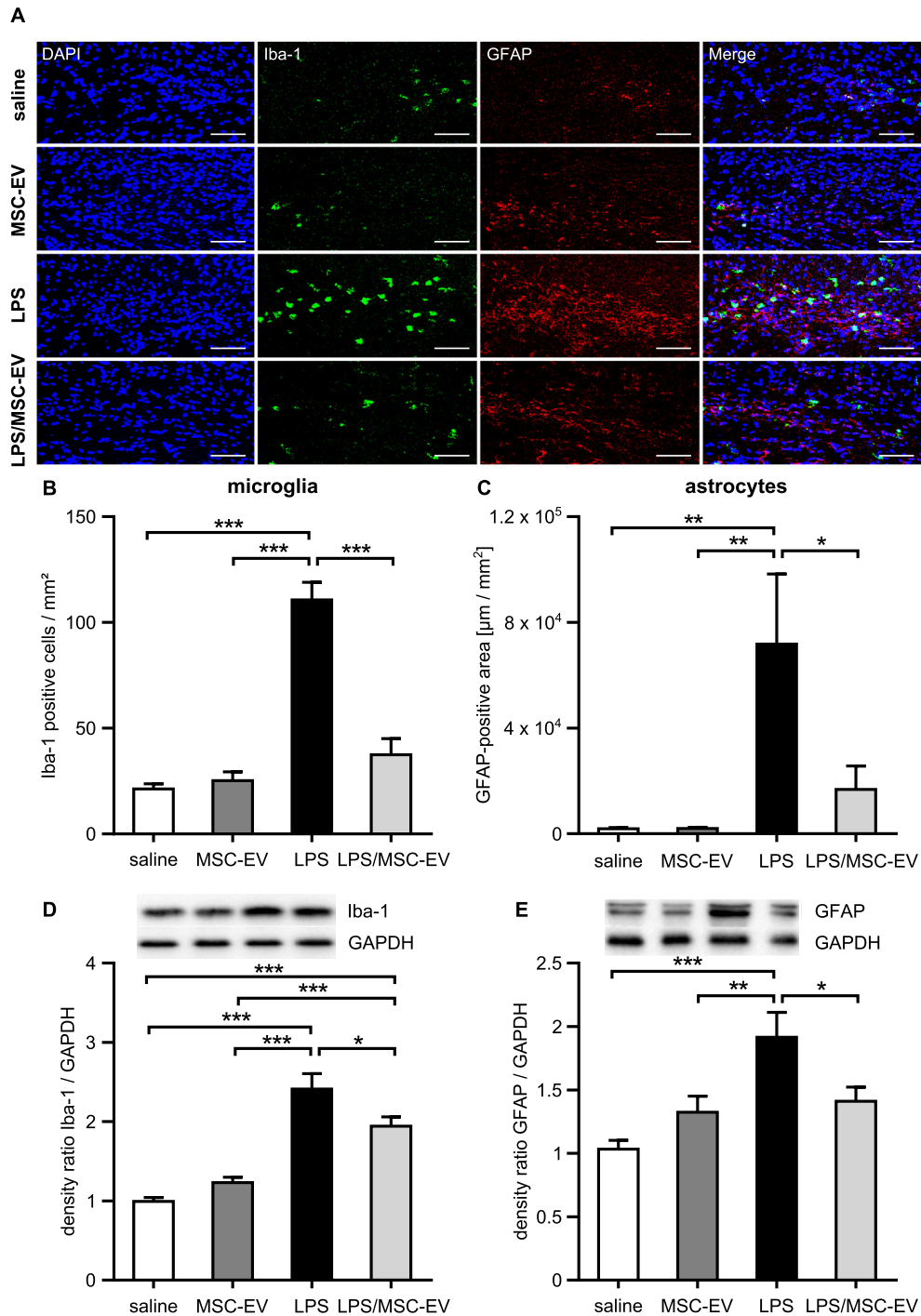


**Fig. 2.** MSC-EV treatment reduces micro- and astrogliosis after inflammation-induced perinatal brain injury. Microglia and astrocyte cell density was assessed via immunohistochemistry and western blot analysis in white matter-enriched protein lysates including cortex and white matter of the corpus callosum, deep cortical white matter, and external capsule of P5 rats after induction of systemic inflammation (0.25 mg/kg LPS, i.p.) at P3. Two repetitive i.p. injections of MSC-EVs were administered at 3 h before and 24 h post LPS-injection. Representative images of microglia (Iba-1) and astrocytes (GFAP) in the cingulate white matter are presented for each treatment group (Scale bar: 100 µm) (A). Density of microglia (B) and astrocytes (C) in the cingulate white matter and the internal capsule was quantified by counting Iba-1 positive cells and by measuring the GFAP-positive area, respectively (n = 7). Protein expression of Iba-1 (D) and GFAP (E) was analysed via Western blot analysis in white matter-enriched brain fractions including cortex, corpus callosum, deep cortical white matter, and external capsule (n = 12–15 per group). Data are presented as mean + SEM. \*p < 0.05, \*\*p < 0.01, \*\*\*p < 0.001.

indicating a time-dependent period of vulnerability in the immature brain (Favrais et al., 2011). In line with these findings, we observed impairment of long-term spatio-temporal memory function and recognition memory deficits in rats injected with LPS at P3. These deficits became evident in adolescent animals as demonstrated by an increased latency to find the escape hole in

the Barnes Maze and by a reduced exploration time in the Novel Object Recognition test. The fact that every animal was subjected to all behavioural tasks (Open Field, Barnes maze, Novel Object Recognition) starting at P30 and P90, respectively, might be a limitation of the current study. Experimental tasks performed at P30 may have altered behaviour in the re-testing session at P90

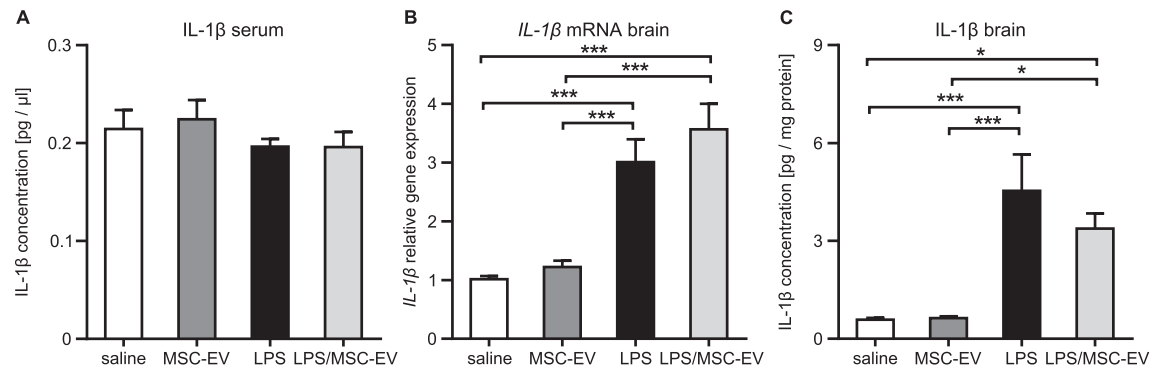


**Fig. 3.** Inflammation induced cytokine response is not altered by MSC-EV treatment. Quantification of systemic and local IL-1 $\beta$  concentrations after exposure to LPS (0.25 mg/kg i.p.) at P3 and two repetitive i.p. injections of MSC-EVs at 3 h before and 24 h post LPS-injection. Pups were sacrificed 48 h after LPS administration and IL-1 $\beta$  protein concentrations were determined in serum (A, n = 5–6). In brain samples cerebral IL1 $\beta$  mRNA expression and protein concentration (B, n = 8–9; C, n = 8–9) were measured. Data are presented as mean + SEM. \* $p$  < 0.05, \*\*\* $p$  < 0.001.

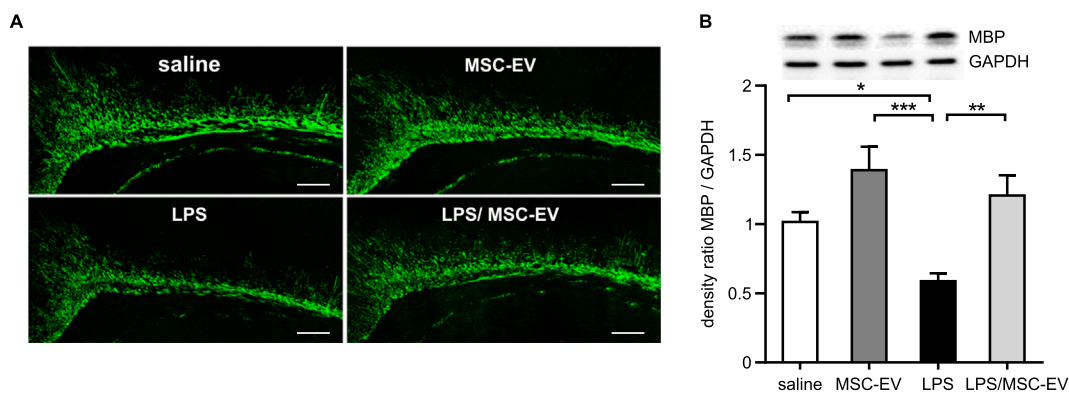


**Fig. 4.** MSC-EV treatment restores inflammation-induced hypomyelination. MBP expression, as a key marker for myelination, was analysed by immunohistochemistry and western blot analysis at P11. Animals were treated with LPS (0.25 mg/kg, i.p.) at P3. MSC-EVs were administered at 3 h before and 24 h post LPS injection. Representative images derived from immunohistochemical staining for MBP (confocal large scale images, bregma: 3.48  $\pm$  0.2 mm) revealed group differences in the white matter (Scale bar: 200  $\mu$ m) (A). Quantification of protein expression analysis of whole hemispheres (cerebellum excluded) by western blot analysis (B, n = 10–15 per group). Data are presented as mean + SEM. \* $p$  < 0.05, \*\* $p$  < 0.01, \*\*\* $p$  < 0.001.

due to learning and forced physical activity at adolescent age which may explain the rather modest effects we observed at P90.

Nevertheless, cognitive impairments at adolescent age were largely ameliorated by administration of MSC-EVs. Clinical observations indicate that alterations of white matter microstructure in preterm infants persist into adulthood and are associated with cognitive dysfunction (Allin et al., 2011). From studies in adult neurodegenerative diseases and traumatic brain injury involving white matter alterations it is further suggested that abnormal myelin remodelling and white matter connectivity modify axonal conduction efficiency and correlate with cognitive dysfunction (Armstrong et al., 2015; Lin et al., 2015). Therefore, we hypothesize that long-term protection on cognitive deficits by MSC-EVs may result from preservation of neonatal LPS-induced disturbed white matter development.

In line with previous preclinical reports the current study reveals that LPS administered at P3 causes acute inflammation involving micro- and reactive astrogliosis associated with cellular degeneration and long-term microstructural alterations of the developing white matter (Brehmer et al., 2012; Lodygensky et al., 2014; Nobuta et al., 2012; Smith et al., 2014). Both, microglia and astrocytes are frequently affected in various types of brain injury and are profoundly activated in white matter lesions of periventricular leukomalacia (Haynes et al., 2003; Lodygensky et al., 2014; Volpe, 2009). Key effector mechanisms of activated microglia and astrocytes include the secretion of pro-

inflammatory cytokines and the production of free radicals thereby enhancing excitotoxicity which finally culminates in injury of white matter components (Volpe, 2009). MSCs have been shown to inhibit LPS-stimulated microglia proliferation *in vitro* by modulating the cytokine response (Jose et al., 2014). Intravenous administration of MSCs reduced the acute inflammatory response in the aforementioned ovine model of intrauterine hypoxia-ischemia, i.e. microgliosis was diminished (Jellema et al., 2013). However, when applying MSC-EVs in the same model no anti-inflammatory capacities were detected suggesting individual differences between experimental settings (Ophelders et al., 2016).

In contrast, immunomodulating activities of MSC-EVs were shown in a murine ischemic stroke model where MSC-EV treatment suppressed stroke associated lymphopenia and improved post-stroke symptoms in the same manner as MSCs, which were the source of the applied MSC-EVs (Doepfner et al., 2015). Furthermore, *in vitro* analyses combined with a clinical treatment attempt in steroid-resistant acute graft-versus-host-disease demonstrated that MSC-EVs suppress inflammatory responses in humans (Kordelas et al., 2014). Also the present findings in our model of inflammatory preterm brain injury revealed that beneficial effects of MSC-EVs on cellular degeneration and hypomyelination were directly associated with reduced gliosis. Importantly, statistical analysis revealed strong interplay between LPS exposure and effect of MSC-EV treatment indicating that EVs exert their full potential upon an inflammatory stimulus. Therefore, it may be hypothesised



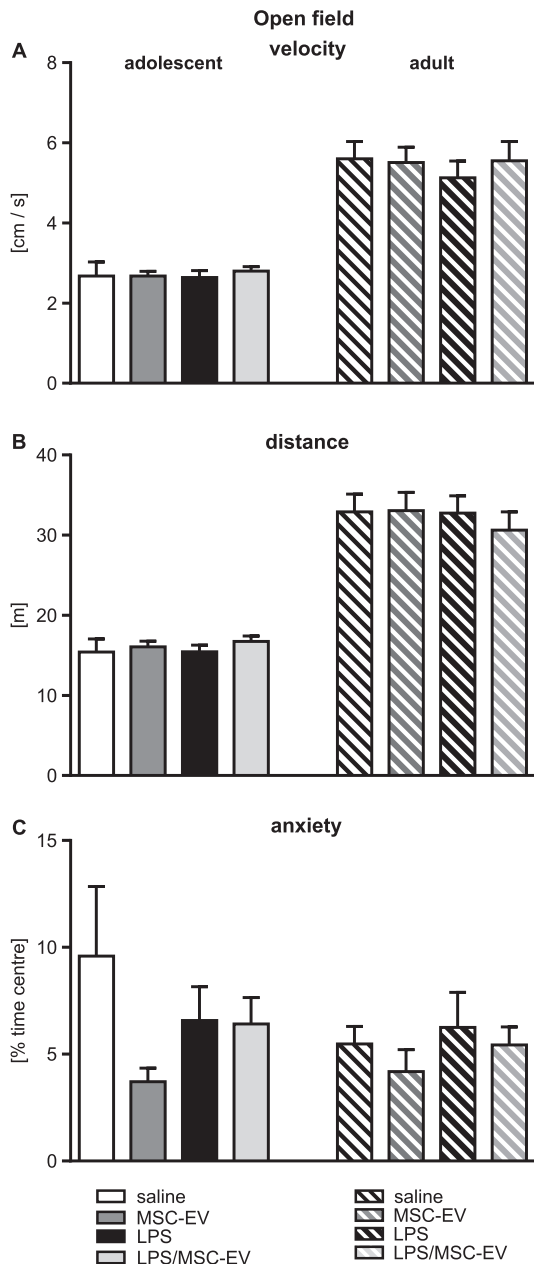


**Fig. 5.** Motor activity and anxiety-related behaviour is not altered after systemic inflammation and MSC-EV treatment. General motor activity measured in the *Open Field* maze expressed by mean velocity (cm/s) (A) and total travelled distance (B) measured at P30 (adolescent) and at P90 (adult) after induction of systemic inflammation (0.25 mg/kg LPS, i.p.) at P3 and MSC-EV treatment at 3 h before and 24 h after LPS injection. Anxiety-related behaviour is illustrated as percent of time the animals spent in the centre region of the *Open Field* arena (C). Data are presented as mean + SEM; \* $p < 0.05$ ; \*\* $p < 0.01$ ; (n = 8–10 per group).

that MSC-EVs exert their neuroprotective effects by modulation of micro- and astroglia activity as major cellular sources of pro-inflammatory cytokines (Kim et al., 2011; Li et al., 2008).

Whether systemically applied EVs directly act in the brain remains unclear. Besides the systemic mode of action (Doepfner et al., 2015; Kordelas et al., 2014), EVs have been suggested to cross the blood brain barrier upon an inflammatory stimulus and deliver RNA-messages to neurons (Ridder et al., 2014). Since LPS is known to induce an acute pro-inflammatory response in both the periphery and the brain analysis of pro-inflammatory cytokines in our experimental setting revealed a marked increase in IL-1 $\beta$  mRNA

and protein expression in the brain at 48 h post LPS injection even though circulating IL-1 $\beta$  levels were not affected. This may be explained by a differential regulation of LPS-induced cytokine responses in the periphery and the brain (Erickson and Banks, 2011). Analyses on TNF $\alpha$  and IL-18 expression by LPS and MSC-EVs in serum and brain revealed only modest effects. However, time points, chosen to correlate findings with our read-outs on cerebral apoptosis and gliosis might have been too late and acute treatment effects on cytokine responses might have resolved (Bilbo et al., 2005; Claypoole et al., 2017; Kendall et al., 2011). Since MSC-EV application did not influence expression of the selected pro-inflammatory cytokines, additional analysis of a broader set of molecules including anti-inflammatory cytokines is needed to explore the impact of MSC-EV on LPS-induced neuroinflammatory responses in detail.

An additional target mechanism of MSC-EVs might be the promotion of regeneration since *in vivo* data showed a remyelinating effect after intracerebral application of MSCs in models of neonatal brain injury (Titomanlio et al., 2011; van Velthoven et al., 2010). We also observed a restoration of myelin structures after systemic MSC-EV treatment, suggesting that in addition to prevention of acute cellular degeneration, myelination was promoted. Keeping the multiple hit hypothesis in the pathogenesis of preterm brain injury in mind, potential neuroprotective agents need to be applied for prevention and also treatment of injury and developmental disturbances (Kaindl et al., 2009). In the present study, the first time point of injection was chosen to secure the full anti-inflammatory potential of MSC-EVs directly at the beginning when the inflammatory cascade is evolving. In line with the current literature (Zhang et al., 2015), an additional dose was administered after 24 h. Moreover, with this treatment regime we aim to mimic the complex clinical situation in preterm infants where exact timing of the injurious insult often remains elusive. However, it is well possible that repetitive therapeutic doses as used by Doepfner and co-workers might even potentiate the regenerative effect (Doepfner et al., 2015). The present study implicates that systemic injection of MSC-EVs is a feasible route of administration and effectively reduces the primary inflammatory response mediated by microglia and has long-term neuroprotective potential against white matter injury.

Even though detailed molecular mechanisms for the described protective potential of MSC-EVs remain to be clarified in further studies, a few key molecules of MSC-EVs have been identified in adult neurodegenerative diseases. For example, it is hypothesised that specific microRNAs are required to mediate the MSC-EVs' neuroprotective effect (Xin et al., 2012). In the future, the detailed characterisation of the MSC-EVs content will be of significant importance to interpret the molecular basis of protection observed in the present disease model (Konala et al., 2016; Lener et al., 2015; Mitsialis and Kourembanas, 2016).

In summary, further pre-clinical characterisation of the therapeutic potential of MSC-EVs for neonatal brain injury seems highly warranted. In addition, translation of MSC-EVs as therapeutic concepts into clinical application as an off-the shelf product requires regulatory categorization within existing frameworks (Börger et al., 2016).

## 6. Conclusion

Since transplantation of undifferentiated cells renders potential risks for treatment of human infants such as proliferation and formation of emboli, MSC-EVs are a promising new therapeutic and regenerative strategy for the developing brain. The findings of the present study suggest that it seems worthwhile to investigate their mechanisms of action in further experimental settings of

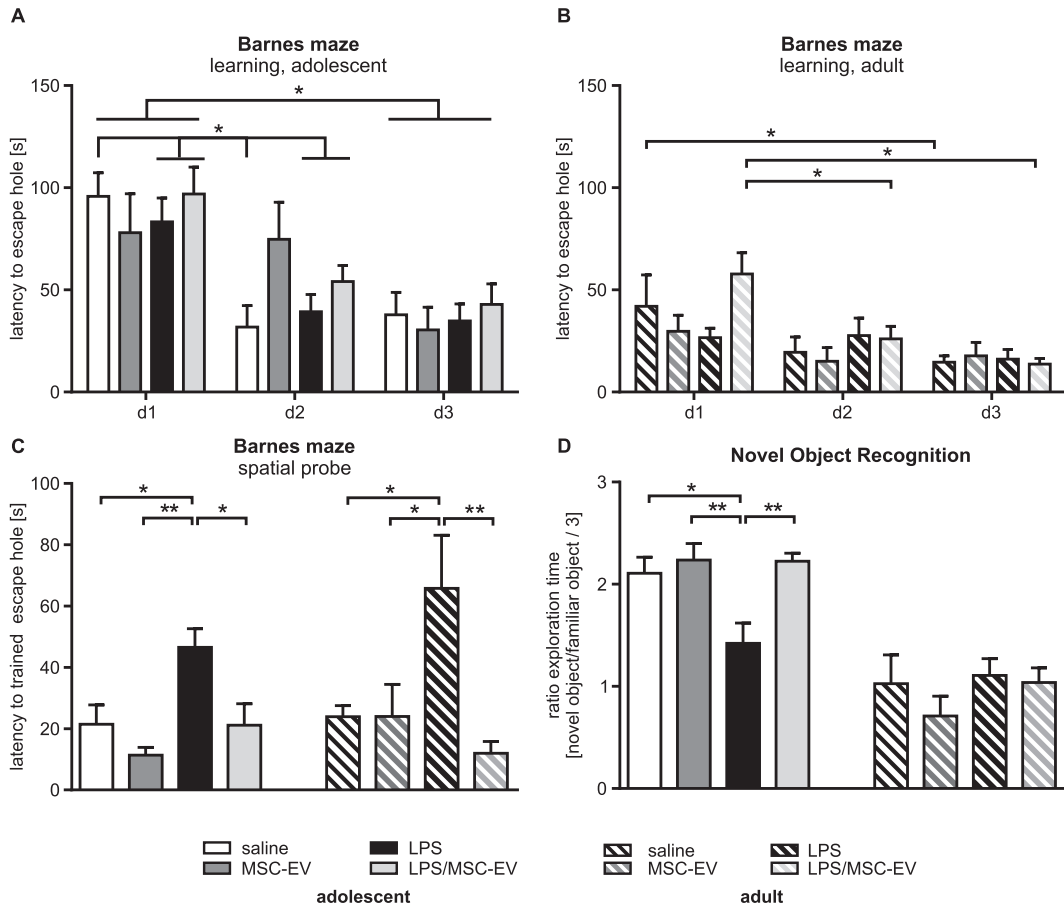


**Fig. 6.** MSC-EVs improve cognitive function after perinatal inflammatory brain injury. Cognitive function and learning behaviour were assessed at P30 (adolescent) and at P90 (adult) after induction of systemic inflammation (0.25 mg/kg LPS, i.p.) at P3. MSC-EVs were administered at 3 h before and 24 h after LPS injection. Learning behaviour was determined over three training days in adolescent (A) and adult (B) animals using the *Barnes Maze* test measuring the latency to find the escape hole. Cognitive function was assessed at the fourth day in the probe trial when all holes of the *Barnes Maze* were closed (C). Effects on cognitive function were further assessed in the *Novel Object Recognition* test measuring exploration times at familiar and novel objects. As a measure of cognitive function the ratio of exploration time at the novel object compared to familiar objects was calculated (D). Data are presented as mean + SEM; \**p* < 0.05; \*\**p* < 0.01; (n = 8–10 per group).

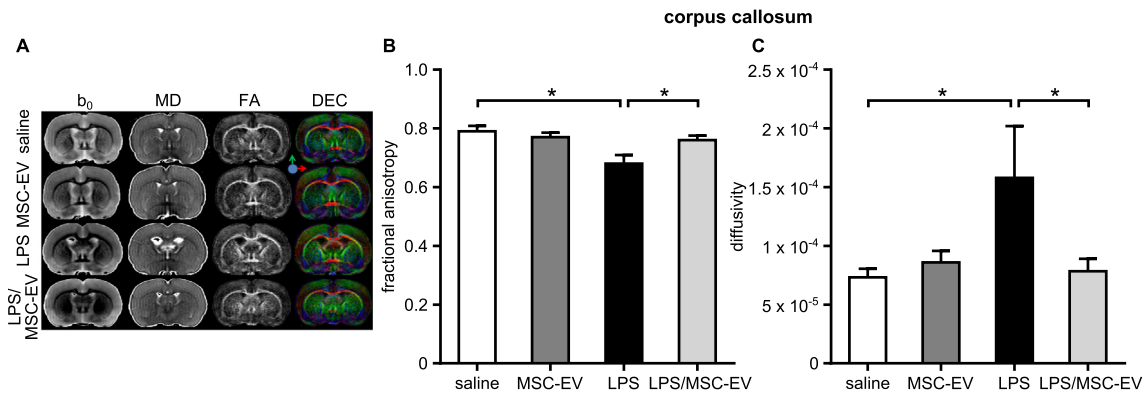


**Fig. 7.** Long-term white matter microstructure development is restored by MSC-EV treatment. Using DT-MRI long-term microstructural white matter alterations were analysed at P125 after neonatal exposure to systemic inflammation (0.25 mg/kg LPS, i.p.) at P3. MSC-EVs were administered at 3 h before and 24 h post LPS injection. Representative illustrations of T<sub>2</sub>W (b<sub>0</sub>) images, mean diffusivity (MD), fractional anisotropy, and direction encoded colour (DEC) maps are shown for each treatment group (A). Fractional anisotropy (B) and radial diffusivity (C) were quantified in the corpus callosum. Data are presented as mean + SEM; \**p* < 0.05; n = 6 per group.

neonatal brain injury and develop their production through the required safety standards to make this promising therapy suitable for clinical trials in infants.

**Disclosure**

The authors indicated no potential conflicts of interest.

## Acknowledgment

This work was supported by the Deutsche Forschungsgemeinschaft (DFG grant Fe 518/5-1, UFM), an IFORES-grant by the Medical Faculty of the University of Duisburg-Essen (KD, BG, JH, UF-M), the Frentzen- and C.D.-Foundation (UFM, IB), the Volkswagen Foundation, and the Kompetenznetzwerk Stammzellforschung NRW (BG), and the CIBM of the UNIL, UNIGE, HUG, CHUV, EPFL, Leenards, and Jeantet foundations (YV). We thank Karina Kempe and Mandana Rizazad for their excellent technical assistance. We also thank Jörg Steinmann for assistance with microbiological analyses.

## Appendix A. Supplementary data

Supplementary data associated with this article can be found, in the online version, at <http://dx.doi.org/10.1016/j.bbi.2016.11.011>.

## References

- Allin, M.P., Kontis, D., Walshe, M., Wyatt, J., Barker, G.J., Kanaan, R.A., McGuire, P., Rifkin, L., Murray, R.M., Nosarti, C., 2011. White matter and cognition in adults who were born preterm. *PLoS ONE* 6, e24525. <http://dx.doi.org/10.1371/journal.pone.0024525>.
- Andrews, W.W., Goldenberg, R.L., Hauth, J.C., 1995. Preterm labor: emerging role of genital tract infections. *Infect. Agents Dis.* 4, 196–211.
- Anjari, M., Counsell, S.J., Srinivasan, L., Allsop, J.M., Hajnal, J.V., Rutherford, M.A., Edwards, A.D., 2009. The association of lung disease with cerebral white matter abnormalities in preterm infants. *Pediatrics* 124, 268–276. <http://dx.doi.org/10.1542/peds.2008-1294>.
- Armstrong, R.C., Mierzwa, A.J., Sullivan, G.M., Sanchez, M.A., 2015. Myelin and oligodendrocyte lineage cells in white matter pathology and plasticity after traumatic brain injury. *Neuropharmacology*. <http://dx.doi.org/10.1016/j.neuropharm.2015.04.029>.
- Baron, F., Storb, R., 2011. Mesenchymal stromal cells: a new tool against graft-versus-host disease? *Biol. Blood Marrow Transplant.* <http://dx.doi.org/10.1016/j.bbmt.2011.09.003>.
- Beck, S., Wojdyła, D., Say, L., Betran, A.P., Merialdi, M., Requejo, J.H., Rubens, C., Menon, R., Van Look, P.F., 2010. The worldwide incidence of preterm birth: a systematic review of maternal mortality and morbidity. *Bull. World Health Organ.* 88, 31–38. <http://dx.doi.org/10.2471/BLT.08.062554>.
- Benders, M.J., Kersbergen, K.J., de Vries, L.S., 2014. Neuroimaging of white matter injury, intraventricular and cerebral hemorrhage. *Clin. Perinatol.* 41, 69–82. <http://dx.doi.org/10.1016/j.clp.2013.09.005>. PMID/Accession number: 24524447.
- Belmonte, M.K., Allen, G., Beckel-Mitchener, A., Boulanger, L.M., Carper, R.A., Webb, S.J., 2004. Autism and abnormal development of brain connectivity. *J. Neurosci.* 24, 9228–9231. <http://dx.doi.org/10.1523/JNEUROSCI.3340-04.2004>.
- Bianco, P., Cao, X., Frenette, P.S., Mao, J.J., Robey, P.G., Simmons, P.J., Wang, C.Y., 2013. The meaning, the sense and the significance: translating the science of mesenchymal stem cells into medicine. *Nat. Med.* 19, 35–42. <http://dx.doi.org/10.1038/nm.3028>.
- Bilbo, S.D., Biedenkapp, J.C., Der-Avakian, A., Watkins, L.R., Rudy, J.W., Maier, S.F., 2005. Neonatal infection-induced memory impairment after lipopolysaccharide in adulthood is prevented via caspase-1 inhibition. *J. Neurosci.* 25, 8000–8009. <http://dx.doi.org/10.1523/JNEUROSCI.1748-05.2005>.
- Börger, V., Bremer, M., Görgens, A., Giebel, B., 2016. Mesenchymal stem/stromal cell-derived extracellular vesicles as a new approach in stem cell therapy. *ISBT Sci. Ser.* 11, 228–234. <http://dx.doi.org/10.1111/vox.12212>.
- Brehner, F., Bendix, I., Prager, S., van de Looij, Y., Reinboth, B.S., Zimmermann, J., Schlager, G.W., Brait, D., Siffringer, M., Endesfelder, S., Sizonenko, S., Mallard, C., Bührer, C., Felderhoff-Mueser, U., Gerstner, B., 2012. Interaction of inflammation and hyperoxia in a rat model of neonatal white matter damage. *PLoS ONE* 7, e49023. <http://dx.doi.org/10.1371/journal.pone.0049023>.
- Bruno, S., Grange, C., Deregius, M.C., Calogero, R.A., Saviozzi, S., Collino, F., Morando, L., Busca, A., Falda, M., Bussolati, B., Tetta, C., Camussi, G., 2009. Mesenchymal stem cell-derived microvesicles protect against acute tubular injury. *J. Am. Soc. Nephrol.* 20, 1053–1067. <http://dx.doi.org/10.1681/ASN.2008070798>.
- Cai, Z., Pan, Z.L., Pang, Y., Evans, O.B., Rhodes, P.G., 2000. Cytokine induction in fetal rat brains and brain injury in neonatal rats after maternal lipopolysaccharide administration. *Pediatr. Res.* 47, 64–72.
- Chambon, C., Wegener, N., Gravius, A., Danysz, W., 2011. A new automated method to assess the rat recognition memory: validation of the method. *Behav. Brain Res.* 222, 151–157. <http://dx.doi.org/10.1016/j.bbr.2011.03.032>.
- Claypoole, L.D., Zimmerberg, B., Williamson, L.L., 2017. Neonatal lipopolysaccharide treatment alters hippocampal neuroinflammation, microglia morphology and anxiety-like behavior in rats selectively bred for an infantile trait. *Brain Behav. Immun.* 59, 135–146.
- Counsell, S.J., Edwards, A.D., Chew, A.T., Anjari, M., Dyet, L.E., Srinivasan, L., Boardman, J.P., Allsop, J.M., Hajnal, J.V., Rutherford, M.A., Cowan, F.M., 2008. Specific relations between neurodevelopmental abilities and white matter microstructure in children born preterm. *Brain* 131, 3201–3208. <http://dx.doi.org/10.1093/brain/awn268>.
- de Hoz, L., Simons, M., 2015. The emerging functions of oligodendrocytes in regulating neuronal network behaviour. *BioEssays* 37, 60–69. <http://dx.doi.org/10.1002/bies.201400127>.
- DeFries, J.C., Hegmann, J.P., Weir, M.W., 1966. Open-field behavior in mice: evidence for a major gene effect mediated by the visual system. *Science* 154, 1577–1579.
- Doepfner, T.R., Herz, J., Gorgens, A., Schlechter, J., Ludwig, A.K., Radtke, S., de Miroshedji, K., Horn, P.A., Giebel, B., Hermann, D.M., 2015. Extracellular vesicles improve post-stroke neuroregeneration and prevent postischemic immunosuppression. *Stem Cells Transl. Med.* 4, 1131–1143. <http://dx.doi.org/10.5966/sctm.2015-0078>.
- Donega, V., Nijboer, C.H., van Tilborg, G., Dijkhuizen, R.M., Kavelaars, A., Heijnen, C.J., 2014. Intranasally administered mesenchymal stem cells promote a regenerative niche for repair of neonatal ischemic brain injury. *Exp. Neurol.* 261, 53–64. <http://dx.doi.org/10.1016/j.expneurol.2014.06.009>.
- Eklind, S., Mallard, C., Leverin, A.L., Gilland, E., Blomgren, K., Mattsby-Baltzer, I., Hagberg, H., 2001. Bacterial endotoxin sensitizes the immature brain to hypoxic-ischaemic injury. *Eur. J. Neurosci.* 13, 1101–1106.
- Erickson, M.A., Banks, W.A., 2011. Cytokine and chemokine responses in serum and brain after single and repeated injections of lipopolysaccharide: multiplex quantification with path analysis. *Brain Behav. Immun.* 25, 1637–1648. <http://dx.doi.org/10.1016/j.bbi.2011.06.006>.
- Favrais, G., van de Looij, Y., Fleiss, B., Ramanantsoa, N., Bonnin, P., Stoltenberg-Didinger, G., Lacaud, A., Saliba, E., Dammann, O., Gallego, J., Sizonenko, S., Hagberg, H., Lelievre, V., Gressens, P., 2011. Systemic inflammation disrupts the developmental program of white matter. *Ann. Neurol.* 70, 550–565. <http://dx.doi.org/10.1002/ana.22489>.
- Felderhoff-Mueser, U., Bittigau, P., Siffringer, M., Jarosz, B., Korobowicz, E., Mahler, L., Piening, T., Moysich, A., Grune, T., Thor, F., Heumann, R., Bührer, C., Ikonomidou, C., 2004. Oxygen causes cell death in the developing brain. *Neurobiol. Dis.* 17, 273–282. <http://dx.doi.org/10.1016/j.nbd.2004.07.019>.
- Gerdoni, E., Gallo, B., Casazza, S., Musio, S., Bonanni, I., Pedemonte, E., Mantegazza, R., Frassonni, F., Mancardi, G., Pedotti, R., Uccelli, A., 2007. Mesenchymal stem cells effectively modulate pathogenic immune response in experimental autoimmune encephalomyelitis. *Ann. Neurol.* 61, 219–227. <http://dx.doi.org/10.1002/ana.21076>.
- Gnecchi, M., He, H., Liang, O.D., Melo, L.G., Morello, F., Mu, H., Noiseux, N., Zhang, L., Pratt, R.E., Ingwall, J.S., Dzau, V.J., 2005. Paracrine action accounts for marked protection of ischemic heart by Akt-modified mesenchymal stem cells. *Nat. Med.* 11, 367–368. <http://dx.doi.org/10.1038/nm0405-367>.
- Hagberg, H., Mallard, C., 2005. Effect of inflammation on central nervous system development and vulnerability. *Curr. Opin. Neurol.* 18, 117–123.
- Haynes, R.L., Folkert, R.D., Keefe, R.J., Sung, I., Swzeda, L.I., Rosenberg, P.A., Volpe, J.J., Kinney, H.C., 2003. Nitrosative and oxidative injury to premyelinating oligodendrocytes in periventricular leukomalacia. *J. Neuropathol. Exp. Neurol.* 62, 441–450.
- Hess, D.C., Hill, W.D., 2011. Cell therapy for ischaemic stroke. *Cell Prolif.* 44 (Suppl. 1), 1–8. <http://dx.doi.org/10.1111/j.1365-2184.2010.00718.x>.
- Hsieh, J.Y., Wang, H.W., Chang, S.J., Liao, K.H., Lee, I.H., Lin, W.S., Wu, C.H., Lin, W.Y., Cheng, S.M., 2013. Mesenchymal stem cells from human umbilical cord express preferentially secreted factors related to neuroprotection, neurogenesis, and angiogenesis. *PLoS ONE* 8, e72604. <http://dx.doi.org/10.1371/journal.pone.0072604>.
- Jellema, R.K., Wolfs, T.G., Lima Passos, V., Zwanenburg, A., Ophelders, D.R., Kuypers, E., Hopman, A.H., Dudink, J., Steinbusch, H.W., Andriessen, P., Germeraad, W.T., Vanderlocht, J., Kramer, B.W., 2013. Mesenchymal stem cells induce T-cell tolerance and protect the preterm brain after global hypoxia-ischemia. *PLoS ONE* 8, e73031. <http://dx.doi.org/10.1371/journal.pone.0073031>.
- Johnson, S., Wolke, D., Hennessy, E., Marlow, N., 2011. Educational outcomes in extremely preterm children: neuropsychological correlates and predictors of attainment. *Dev. Neuropsychol.* 36, 74–95. <http://dx.doi.org/10.1080/87565641.2011.540541>.
- Jose, S., Tan, S.W., Ooi, Y.Y., Ramasamy, R., Vidyadaran, S., 2014. Mesenchymal stem cells exert anti-proliferative effect on lipopolysaccharide-stimulated BV2 microglia by reducing tumour necrosis factor- $\alpha$  levels. *J. Neuroinflamm.* 11, 149. <http://dx.doi.org/10.1186/s12974-014-0149-8>.
- Kaindl, A.M., Favrais, G., Gressens, P., 2009. Molecular mechanisms involved in injury to the preterm brain. *J. Child Neurol.* 24, 1112–1118. <http://dx.doi.org/10.1177/0883073809337920>.
- Karen, T., Schlager, G.W., Bendix, I., Siffringer, M., Herrmann, R., Pantazis, C., Enot, D., Keller, M., Kerner, T., Felderhoff-Mueser, U., 2013. Effect of propofol in the immature rat brain on short- and long-term neurodevelopmental outcome. *PLoS ONE* 8, e64480. <http://dx.doi.org/10.1371/journal.pone.0064480>.
- Kendall, G.S., Hristova, M., Horn, S., Dafou, D., Acosta-Saltos, A., Almolda, B., Zbarsky, V., Rumajogee, P., Heuer, H., Castellano, B., Pfeffer, K., Nedospasov, S.A., Peebles, D.M., Raivich, G., 2011. TNF gene cluster deletion abolishes lipopolysaccharide-mediated sensitization of the neonatal brain to hypoxic ischemic insult. *Lab. Invest.* 91, 328–341. <http://dx.doi.org/10.1038/labinvest.2010.192>.



- Yanez-Mo, M., Siljander, P.R., Andreu, Z., Zavec, A.B., Borrás, F.E., Buzas, E.I., Buzas, K., Casal, E., Cappello, F., Carvalho, J., Colas, E., Cordeiro-da Silva, A., Fais, S., Falcon-Perez, J.M., Ghobrial, I.M., Giebel, B., Gimona, M., Graner, M., Gursel, I., Gursel, M., Heegaard, N.H., Hendrix, A., Kierulf, P., Kokubun, K., Kosanovic, M., Kralj-Iglic, V., Kramer-Albers, E.M., Laitinen, S., Lasser, C., Lener, T., Ligeti, E., Line, A., Lipps, G., Llorente, A., Lotvall, J., Mancek-Keber, M., Marcilla, A., Mittelbrunn, M., Nazarenko, I., Nolte-'t Hoen, E.N., Nyman, T.A., O'Driscoll, L., Olivan, M., Oliveira, C., Pallinger, E., Del Portillo, H.A., Reventos, J., Rigau, M., Rohde, E., Sammar, M., Sanchez-Madrid, F., Santarem, N., Schallmoser, K., Ostenfeld, M.S., Stoorvogel, W., Stukelj, R., Van der Grein, S.G., Vasconcelos, M. H., Wauben, M.H., De Wever, O., 2015. Biological properties of extracellular vesicles and their physiological functions. *J. Extracellular Vesicles* 4, 27066. <http://dx.doi.org/10.3402/jev.v4.27066>.
- Zhang, Y., Chopp, M., Meng, Y., Katakowski, M., Xin, H., Mahmood, A., Xiong, Y., 2015. Effect of exosomes derived from multipotent mesenchymal stromal cells on functional recovery and neurovascular plasticity in rats after traumatic brain injury. *J. Neurosurg.* 122, 856–867. <http://dx.doi.org/10.3171/2014.11.JNS14770>.